2024 IEEE/RSJ International Conference on Intelligent Robots and Systems (IROS)
October 14-18, 2024. Abu Dhabi, UAE

FOCWS: A High Sensitive Flexible Optical Curvature Sensor Inspired by Arthropod Sensory Systems

Jiachen Wei[1,2], Zhengwei Li[2,3], Zeyu Liu[2,3], Wei He[1], Long Cheng[2,3], Yanhong Liu[4]

Abstract— **Flexible sensors for joint angle measurement play a crucial role in various human-robot interaction applications. In previous studies, sensors with various sensing mechanisms have been developed. Among them, optical waveguide sensors exhibit high resistance to environmental factors (such as temperature and humidity) and low sensitivity to electromagnetic interference. Researchers have enhanced the sensitivity of optical waveguide sensors to tensile strain by doping other substances (such as graphite) into the optical core material of the optical waveguide. However, the sensitivity of measuring joint angles based on tensile strain principles remains relatively low. In nature, arthropods utilize crack-like structures near their leg joints to perceive minute mechanical stress changes. Here, we propose a curvature sensor based on a Flexible Optical Crack Waveguide Structure (FOCWS) inspired by the arthropod sensory systems. By cutting the optical core, we increase its light power loss during bending strain, thereby enhancing the sensor's sensitivity to angle measurement. The characteristics of light propagation and geometric parameters were studied through simulation, and experiments were designed to validate the simulation results. The average sensitivity is 0.068 dB/°, which is nearly 300 times higher compared to uncut optical waveguide.**

I. INTRODUCTION

Over the past decade, flexible sensors have gained considerable attention for applications in wearable devices [1], [2], human-computer interaction [3]–[6], IoT [7], artificial skin [8], and more. Their flexibility offers unique advantages. Joint angle measurement sensors, a key technology, are widely used in healthcare [9], [10], robotics [5], and virtual reality [11].

Various sensing mechanisms have been used in flexible joint angle sensors, including electrical changes in resistance [12], [13] and capacitance [14], [15], and optical changes in light intensity [16], frequency [17], and wavelength [18], [19]. Strain sensors based on electromagnetic properties are popular due to their simplicity and ease of fabrication, but they are sensitive to environmental electromagnetic fields. Optical sensing methods offer higher sensitivity, robustness, and low susceptibility to electromagnetic interference [20]. While frequency and wavelength detection require costly and bulky instruments like lasers and spectrometers, light intensity sensors are cheaper, smaller, and easily fabricated using photodiodes, LEDs, and waveguides [21]–[23], making them suitable for integration into robotic systems.

Many strain sensors using optical waveguides rely on a single material for the optical core, such as PDMS, which can result in low sensitivity due to minimal light power loss during stretching or bending. To address this, extensive research has focused on enhancing the optical core material. For example, Yang *et al.* (2017) doped PDMS with dye and analyzed its absorption characteristics [24], while Sheng *et al.* (2019) incorporated graphene into PDMS to detect tensile strain through optical loss [25]. Although these methods improved sensitivity to tensile strain, measuring joint angles still presents challenges. Therefore, a new sensor design is needed to enhance sensitivity to angular strain.

Arthropods have crack-like slit organs that can detect tiny mechanical stress changes by contracting or expanding. For example, the slit organ near spider leg joints, shown in Fig. 1(a), serves this function. Inspired by this, we propose a curvature sensor using a Flexible Optical Crack Waveguide Structure (FOCWS), illustrated in Fig. 1(b). By introducing several cracks into the optical core to mimic the slit organ's geometry, this design enhances the waveguide's angle measurement range and sensitivity.

We investigated the FOCWS's response to bending strain under various cutting conditions. The increased light power loss is primarily due to crack formation from cutting. Compared to uncut optical waveguides, the FOCWS's average sensitivity to bending improves by up to nearly 300 times. Additionally, the FOCWS shows excellent dynamic response for detecting bending angles at human hand joints.

This paper is organized as follows: Section II introduces the principles of the FOCWS, Section III describes the design of the FOCWS and presents simulation experiments, Section IV introduces the fabrication method of the FOCWS. In Section V, we validate the simulation results from Section III through experimental verification and we apply the FOCWS to measure angles of human hand joints. Finally, Section VI discusses the limitations of the study and proposes future works.

II. WORKING PRINCIPLE

The FOCWS exploits the mechanism of total internal reflection in optical waveguides, which arises from the different

This work was supported by National Key Research and Development Program of China (Grant No. 2022YFC3602701), National Natural Science Foundation of China (Grant Nos. 62025307 and 62333023), Beijing Nova Program (Grant No. 20230484400), and Beijing Municipal Natural Science Foundation (Grant No. L243014).

[1]School of Intelligence Science and Technology and the Institute of Artificial Intelligence, University of Science and Technology Beijing, Beijing 100083, China.

[2]State Key Laboratory of Multimodal Artificial Intelligence Systems, Institute of Automation, Chinese Academy of Sciences, Beijing 100190, China. Email: long.cheng@ia.ac.cn.

[3]School of Artificial Intelligence, University of Chinese Academy of Sciences, Beijing 100049, China.

[4]School of Electrical and Information Engineering, Zhengzhou University, Zhengzhou, 450001, China.

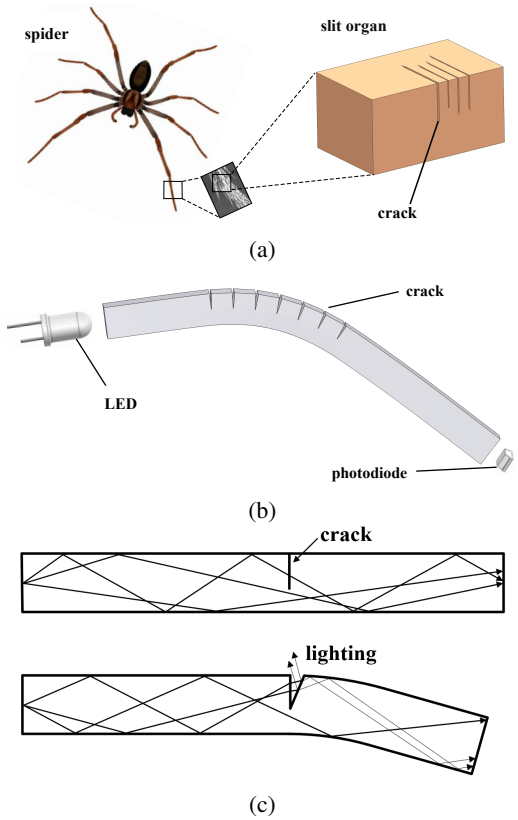

Fig. 1: (a) The schematic depiction of the slit organ found in spiders near the articulation of the tibia and tarsus; (b) Illustration of the FOCWS; (c) The schematic diagrams for the working principle.

refractive indices of the optical core and cladding materials. When the angle of incidence of light from the source to the optical core boundary exceeds the critical angle, total internal reflection occurs. Considering an example, where the refractive index of the cladding material is represented as n_l and the refractive index of the optical core material is n. The condition for total internal reflection at the interface is expressed as:

$$\sin\theta \geq \frac{n_l}{n}. \tag{1}$$

As long as the refractive index of the cladding is lower than that of the optical core, light emitted by the LED can propagate through the optical core through total internal reflection and reach the photodiode. Subsequently, the intensity of light can be measured using the photodiode. However, as depicted in Fig. 1 (c), when the FOCWS undergoes physical deformation, a portion of the light conducted within the optical core may exit the crack, resulting in a reduction in the amount of light traversing through the optical core and causing light power loss. The definition of light power loss is provided below. Consequently, variations in the voltage drop across the photodiode can be detected.

$$L = -10\log_{10}\frac{P}{P_0}, \tag{2}$$

where L represents the power loss, P denotes the light power under deformation and P_0 represent the light power without deformation. The equation indicates that in the absence of deformation, the light power loss is zero, and the power loss increases with an increase in deformation. The sensitivity of the FOCWS can be defined as the change of light power loss with respect to the change of the deformation angle.

III. DESIGN OF THE WAVEGUIDE

In this section, the design of the FOCWS will be discussed. Based on the description of the working principle in the previous section, it can be observed that light power loss occurs at the crack of the FOCWS. Therefore, the light power loss characteristics at the crack were investigated as a primary focus. Subsequently, important geometric parameters were studied with simulation. To reduce the volume of the FOCWS, We take the air as a cladding.

A. The light power loss at the crack

The most significant feature of the FOCWS is the area of the crack. When light propagates in the optical core, encountering a deformed crack causes some light to exit the optical core, resulting in light power loss. In the experiments, the cracks are cut perpendicular to the optical core, so the effect of the crack area on the sensor performance is investigated by varying the size of the cutting depth.

To illustrate the power loss at the crack, we conducted simulation experiments using COMSOL Multiphysics (Fig. 2) to calculate the influence of different cutting depths on the light power loss of the light emitted by the LED in the FOCWS. The LED can be considered as a cone-shaped scattering light source with a cone angle of 30° and a curvature radius of 15 mm. The optical core dimensions are 3 mm × 3 mm × 40 mm. Since the optical core is directly exposed to air, the refractive indices of the optical core material and cladding material are 1.35 and 1.00029, respectively. The refractive index of the optical core material was determined using the laser angle measurement method.

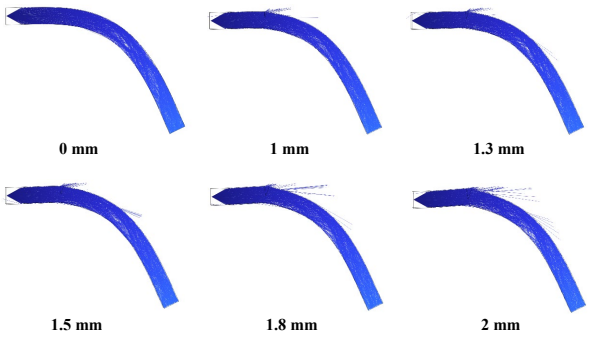

Fig. 2: The optical path in the FOCWS at different cutting depths when the FOCWS is bent by 60°.

The simulation results are depicted in Fig. 3. The results demonstrate that the presence of cracks increases the optical efficiency loss of the waveguide during bending, indicating that larger areas result in greater light power loss at the crack for the same degree of deformation.

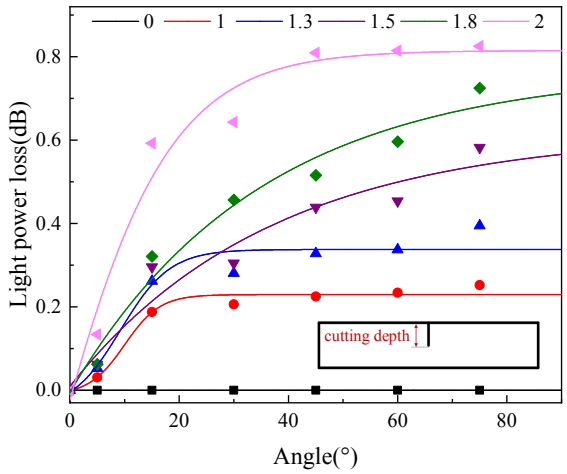

Fig. 3: The relationship between light power loss and bending angle in FOCWS with different cutting depths.

B. Geometric parameters

The previous subsection demonstrated that changing the cutting depth can alter the sensitivity of the waveguide to bending angles. However, the sensitivity enhancement of a single crack on the waveguide is limited, and the measurement range of the waveguide is small. Therefore, it is necessary to increase the number of cracks on the optical core. In this subsection, we focus on analyzing the impact of different combinations of cutting depths and intervals on the relationship between optical power loss and bending angle.

Five models have been designed, each consisting of 7 cracks. These include three models with a cutting depth of 1.5 mm and cutting intervals of 2 mm, 3 mm, and 4 mm, respectively, as well as two models with a cutting interval of 3 mm and cutting depths of 1 mm and 2 mm. As shown in Fig. 4, the FOCWS bends starting from the first crack, adhering closely to a semi-circular model. Optical simulation experiments are conducted throughout the bending process.

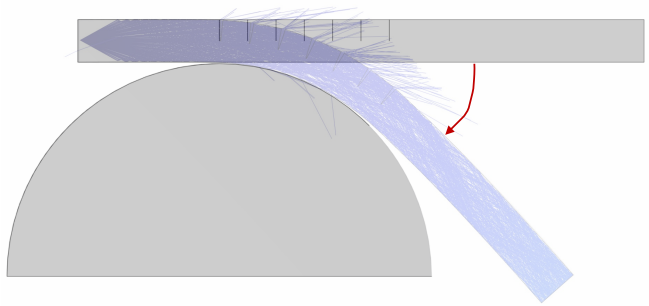

Fig. 4: The schematic diagram of the simulation experiment.

The simulation results, as shown in Fig. 5, indicate that with increasing cutting depth, the light power loss caused by the same angle change becomes greater, resulting an increase in the sensitivity of the waveguide. As the cutting interval increases, the FOCWS's light power loss requires a larger angle to reach saturation, thus expanding the effective

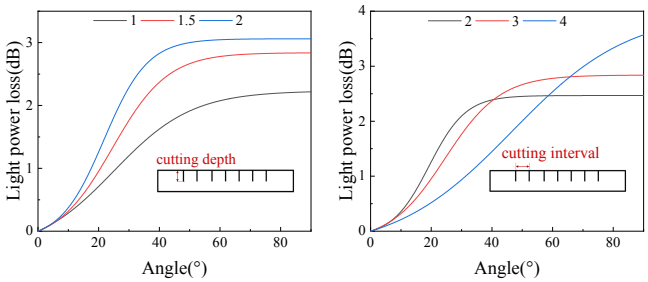

Fig. 5: (a) Cutting intervals of 3 mm with cutting depths of 1 mm, 1.5 mm, and 2 mm; (b) Cutting depth of 1.5 mm with cutting intervals of 2 mm, 3 mm, and 4 mm.

range of measurable angles. However, sensitivity is lower at smaller angles. The range of angle measurement can also be adjusted by varying the number of cuts. Therefore, we choose a smaller cutting interval and the cutting depth can be adjusted as needed.

According to the simulation results above, it can be found that by varying the cutting depth and cutting interval, it is theoretically possible to establish a linear relationship between light power loss and bending angle. This will be further discussed later on.

IV. Fabrication Process

In this section, we will introduce the manufacturing process of the FOCWS. All molds used in the experiment were produced through 3D printing (Markforged X7) with an accuracy of 0.01 mm.

The main step in the production of the sensor is the treatment of the optical core. In this experiment, the optical core material chosen is TPU with a Shore A hardness of 80 (manufactured by Hongsheng Plastic Co., Ltd.). As shown in Fig. 6, after solidification in a 100 mm $\times$ 100 mm $\times$ 3 mm mold, the TPU is laser-cut into specifications of 100 mm $\times$ 3 mm $\times$ 3 mm to serve as the optical core. Next, the optical core is placed into the 3D-printed mold, and then the blade is used to cut along the gap left in the mold, resulting in incisions on the optical core with the same depth and spacing as designed in the mold. Subsequently, the LED (F5-Bullet) and the photodiode (ADPS-9002, Avago Inc) are fixed at both ends of the optical core.

The diameter and length of the optical fiber core affect the sensor's sensitivity and are limited by electronic component specifications. Using smaller photodetectors and surface-mount LEDs can make the sensor more lightweight and flexible. The high hardness of the optical fiber core results in low longitudinal extensibility and reduced lower hysteresis.

V. Experiment Validation

To evaluate the performance of the FOCWS, we designed an motor rotating platform for experimentation. The electric motor rotating platform is shown in Fig. 7. The model of the motor is FAULHABER Series 1524T012S R, which supports real-time feedback of the rotation angle.

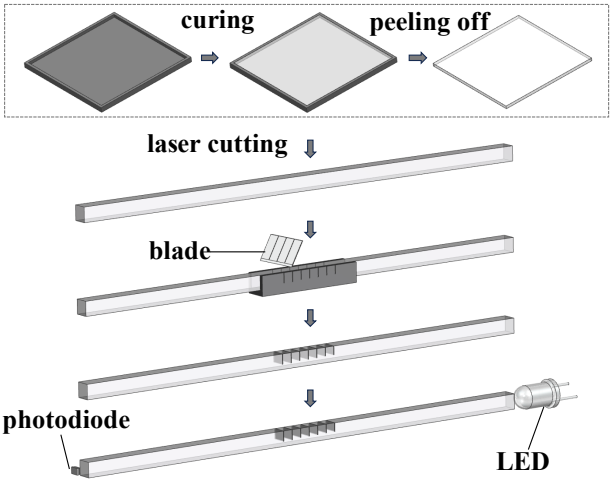

Fig. 6: The schematic diagrams for the fabrication process.

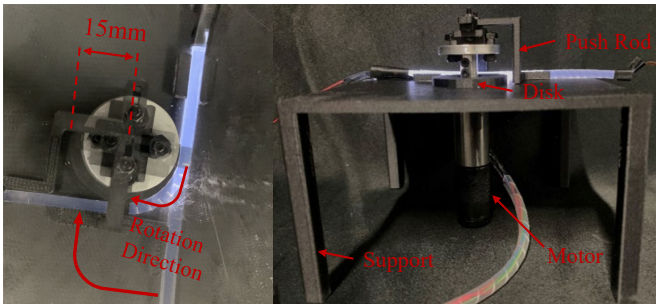

Fig. 7: Top view and front view of the motor rotation platform.

The motorized rotary platform is controlled by a computer that collects real-time rotation angle feedback and photodiode voltage signals (100Hz) from the data acquisition board. This data helps calibrate the voltage-angle relationship. The data acquisition board uses a Type-C interface for power and data transfer.

A. *Testing of the light power loss in the waveguide*

To evaluate the light power loss in the FOCWS, the motor rotation platform was programmed to drive the FOCWS to bend within the range of 0-90°. During each test, the waveguide was placed in the same position.

It was observed during the experiment that the brightness of the LED would affect the response of the FOCWS. In the next subsection, the brightness of the LED will be studied. In this subsection, the brightness of the LED remained constant, and the voltage was maintained at 2.7 V.

The results are shown in Fig. 8 (a). The difference between experimental and simulation results is attributed to the high hardness of the optical core, resulting in the optical core not closely adhering to the axis of rotation during bending.

Fig. 8 (b)(c) shows the response of FOCWS with different cutting depths and cutting intervals to changes in angle. Under the current LED brightness, the FOCWS does not exhibit obvious saturation. The overall trend is consistent with the simulation results (Fig. 5).

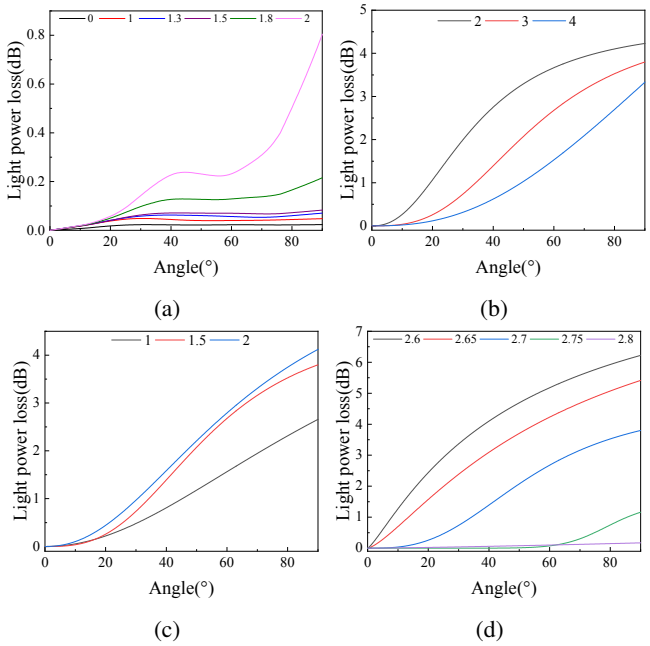

Fig. 8: (a) The response to changes in angle for FOCWS with different cutting depths; (b) Cutting intervals of 3 mm with cutting depths of 1 mm, 1.5 mm, and 2 mm; (c) Cutting depth of 1.5 mm with cutting intervals of 2 mm, 3 mm, and 4 mm; (d) The response of the FOCWS under different LED brightness levels.

B. *The impact of varying LED brightness*

The sensitivity of the FOCWS is also influenced by the brightness of the LED. To examine the impact of brightness on the FOCWS, we conducted tests on a FOCWS with a 3 mm interval between cracks, where all cracks have a depth of 1.5 mm, using voltages of 2.6 V, 2.65 V, 2.7 V, 2.75 V, and 2.8 V.

The sensitivity test under different LED brightness levels is shown in Fig. 8 (d). As the LED brightness increases, the average sensitivity of the FOCWS gradually decreases. When the LED brightness reaches a certain level, the photodiode exhibits saturation. Considering the influence of ambient light and sensor sensitivity, the LED voltage was set to 2.65 V.

C. *Linearity*

To investigate the linear relationship between light power loss in the FOCWS and angle, we designed a model with intervals of 2 mm and sequential crack depths of 2 mm, 2 mm, 1.8 mm, 1.8 mm, 1.7 mm, 1.7 mm and 1.7 mm. The simulation results and experiment results are shown in Fig. 9. Although the results do not exhibit a strictly linear relationship, they indicate that the waveguide structure can achieve a linear relationship between optical power loss and angle while maintaining high sensitivity.

The average sensitivity of the FOCWS reaches 0.068 dB/°, which is nearly 300 times higher compared to the uncut waveguide (Fig. 8 (a) black). Table 1 compares FCOWS with

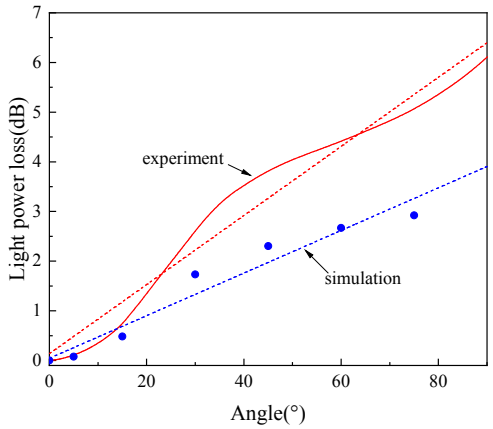

Fig. 9: The simulation results and the experiment results

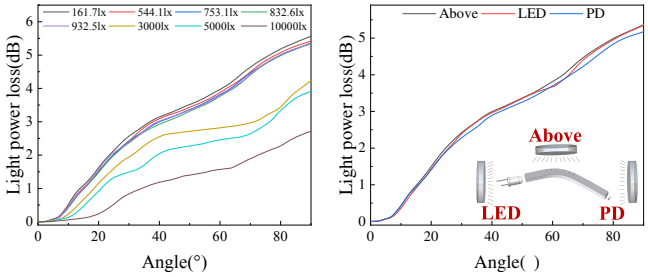

(a) (b)

Fig. 11: (a) The response of the FOCWS under different intensities of ambient light; (b) The response of the FOCWS when ambient light is positioned directly above the FOCWS, at the LED side, and at the PD side.

sensors detecting hand joint angles based on tensile strain. The average sensitivity, calculated using the same method as this paper, shows FCOWS has the highest sensitivity.

TABLE I: Performance results of different sensors

Reference	Sensor type	Stretchability [%]	Linearity	Senitivity
FOCWS[This Work]	Optical	-	Linear	0.068 dB/°
Ref. [18]	Optical	100	Nonlinear	0.014 dB/°
Ref. [12]	Resistive	500	Nonlinear	0.053 dB/°
Ref. [14]	Capacitive	140	Nonlinear	0.005 dB/°
Ref. [13]	Resistive	120	Nonlinear	0.038 dB/°
Ref. [19]	Optical	300	Nonlinear	0.027 dB/°

D. Durability

Durability and stability are crucial for flexible devices. We conducted repetitive experiments on the FOCWS using a motorized rotation platform, allowing the FOCWS to repeat motion between 0-90°. The results are shown in Fig. 10.

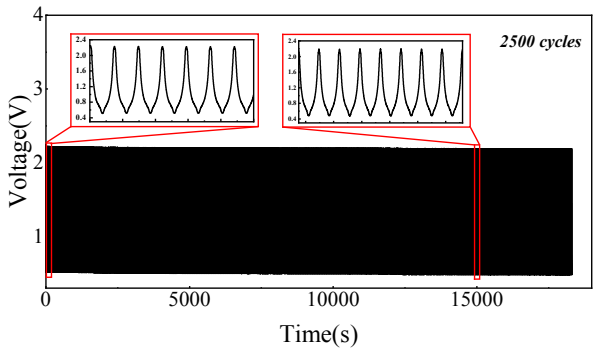

Fig. 10: The repeatability experiments were conducted for 5 hours with 2500 repetitions between 0-90°

The FOCWS demonstrated excellent durability, maintaining its output voltage without decrease even after 2500 cycles, indicating long-term reliability.

E. The influence of ambient light

To evaluate the impact of ambient light on the FOCWS, we controlled the intensity of ambient light by adjusting the distance between another LED light source and the FOCWS, and measured the intensity of ambient light using a digital light meter (TASi, TA632B).

In a brightly lit indoor environment (161.7 lx), the LED light source was placed directly above the FOCWS, and the distance between the LED and the FOCWS was continuously adjusted. The results, as shown in Fig. 11 (a), indicate that the influence of ambient light within the range of 1000 lx on the sensitivity of the FOCWS is limited. Then, the LED light source was placed separately at each end of the FOCWS to assess the impact of ambient light in the tilted direction on the FOCWS. At this point, the light intensity at the waveguide was measured to be 753.1 lx. Fig. 11 (b) illustrates that in a brightly lit indoor environment, ambient light has almost no effect on the sensitivity of the FOCWS. However, as the light intensity continues to increase, the sensitivity of the FOCWS undergoes changes. Nonetheless, if the FOCWS is enclosed, it can also resist ambient light.

F. Application

The FOCWS designed in this study can be mounted on different parts of the body to detect motion performance. To further demonstrate the reliability and practicality of the FOCWS, we attached it to a human hand to measure the bending angle at the joints. As shown in Fig. 12, as the MCP joint bends, the voltage of the sensor decreases. The dynamic response of the FOCWS proves its feasibility for practical applications.

VI. Conclusion and Future Works

This paper introduces a Flexible Optical Crack Waveguide Structure (FOCWS). Through simulations, the characteristics of light propagation and the influence of geometric parameters are studied, and experiments are designed to validate the simulation results. The experiments demonstrate that by simply adjusting the geometric parameters, the FOCWS can simultaneously achieve a large angle measurement range and a high average sensitivity of 0.068 dB/°, with light power loss exhibiting a nearly linear relationship with angle variation. Compared to uncut waveguides, the average sensitivity is increased by nearly 300 times. The method of treating the

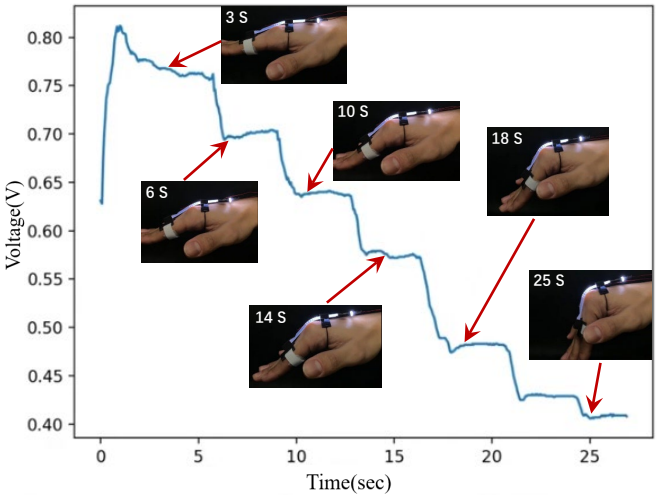

Fig. 12: The change in voltage values of the FOCWS as the human hand joints bend.

optical core described in this paper can be readily applied to other optical waveguides to enhance their sensitivity during bending processes.

Regarding the mentioned issue of slight discrepancies between experimental and simulation results attributed to the high hardness of the optical core. Lowering the hardness of the optical core may introduce other issues, such as the weak adhesion of flexible optical cores. To address these issues, future research will focus on reducing the dimensions of the optical core, miniaturizing the FOCWS to enhance its applicability, and designing cladding to improve stability. Currently, the sensor can only detect deformation in one direction. Future work will involve adding additives and dyes to the core material to enable detection of multi-directional deformation.

REFERENCES

[1] S. Li, X. Zhou, Y. Dong, and J. Li, "Flexible self-repairing materials for wearable sensing applications: Elastomers and hydrogels," *Macromolecular Rapid Communications*, vol.41, no.23, pp.2000444, 2020.

[2] Y. Ling, T. An, L.W. Yap, B. Zhu, S. Gong, and W. Cheng, "Disruptive, soft, wearable sensors," *Advanced Materials*, vol. 32, no. 18, pp. 1904664, 2020.

[3] A. Tashakori, Z. Jiang, A. Servati, S. Soltanian, H. Narayana, K. Le, C. Nakayama, C.-L. Yang, Z.J. Wang, J.J. Eng, and P.Servati, "Capturing complex hand movements and object interactions using machine learning-powered stretchable smart textile gloves," *Nature Machine Intelligence*, pp.1-13, 2024.

[4] T. Kim, S. Lee, T. Hong, G. Shin, T. Kim, and Y. Park, "Heterogeneous sensing in a multifunctional soft sensor for human-robot interfaces," *Science Robotics*, vol. 5, no. 49, 2020, art. no. eabc6878.

[5] H. Wang, W. Wang, J.J. Kim, C. Wang, Y. Wang, B. Wang, S. Lee, T. Yokota, and T. Someya, "An optical-based multipoint 3-axis pressure sensor with a flexible thin-film form," *Science Advances*, vol. 9, no. 36, 2023, art. no. eadi2445.

[6] Z. Li, L. Cheng, and Z. Liu, "Intentional blocking based photoelectric soft pressure sensor with high sensitivity and stability," *Soft Robotics*, vol. 10, no. 1, pp. 205-216, 2023.

[7] A. Kamyshny, S. Magdassi, "Conductive nanomaterials for 2D and 3D printed flexible electronics," *Chemical Society Reviews*, vol. 48, no. 6, pp. 1712-1740, 2019.

[8] Q. Su, Q. Zou, Y. Li, Y. Chen, S.-Y. Teng, J.T. Kelleher, R. Nith, P. Cheng, N. Li, W. Liu, S. Dai, Y. Liu, A. Mazursky, J. Xu, L. Jin, P. Lopes, and S. Wang, "A stretchable and strain-unperturbed pressure sensor for motion interference-free tactile monitoring on skins," *Science Advances*, vol. 7, no. 48, 2021, art. no. eabi4563.

[9] M. Laffranchi, N. Boccardo, S. Traverso, L. Lombardi, M. Canepa, A. Lince, M.Semprini, J.A. Saglia, A. Naceri, R. Sacchetti, E. Gruppioni, and L.D. Michieli, "The Hannes hand prosthesis replicates the key biological properties of the human hand," *Science Robotics*, vol. 5, no. 46, 2020, art. no. eabb0467.

[10] Y. Roh, M. Kim, S.M Won, D. Lim, I. Hong, S. Lee, T. Kim, C. Kim, D. Lee, S. Im, G. Lee, D. Kim, D. Shin, D. Gong, B. Kim, S. Sim, S. Kim, H.K. Kim, B.-K. Koo, J.-S. Kon D. Kang, and S. Han, "Vital signal sensing and manipulation of a microscale organ with a multifunctional soft gripper," *Science Robotics*, vol. 6, no. 59, 2021, art. no. eabi6774.

[11] M. Ortiz-Catalan, J. Zbinden, J. Millenaar, D. D'accolti, M. Controzzi, F. Clemente, L. Cappello, E.J. Earley, E. Mastinu, J. Kolankowska, M. Munoz-Novoa, S. Jonsson, C. Cipriani, P. Sassu, and R. Branemark, "A highly integrated bionic hand with nerual control and feedback for use in daily life," *Science Robotics*, vol. 8, no. 83, 2023, art. no. eadf7360.

[12] M. Amjadi, Y.J. Yoon, and I. Park, Ultra-stretchable and skin-mountable strain sensors using carbon nanotubes-Ecoflex nanocomposites, Nanotechnology, vol. 26, no. 37, pp. 375501, 2015.

[13] X. Guo, Y. Huang, Y. Zhao, L. Mao, L. Gao, W. Pan, Y. Zhang, and P. Liu, Highly stretchable strain sensor based on SWCNTs/CB synergistic conductive network for wearable human-activity monitoring and recognition, Smart Materials and Structures, vol. 26, no. 9, pp.095017, 2017.

[14] R. Nur, N. Matsuhisa, Z. Jiang, M.O.G. Nayeem, T. Yokota, and T. Someya, A highly sensitive capacitive-type strain sensor using wrinkled ultrathin gold films, Nano Letters, vol. 18, no. 9, pp. 5610-5617, 2018.

[15] R.P. Rocha, P.A. Lopes, A.T.d. Almeida, M. Tavakoli, and C. Majidi, "Fabrication and characterization of bending and pressure sensors for a soft prosthetic hand," *Journal of Micromechanics and Microengineering*, vol. 28, no. 3, pp. 034001, 2018.

[16] H. Zhao, K. O'brien, S. Li, and R.F. Shepherd, "Optoelectronically innervated soft prosthetic hand via stretchable optical waveguides," *Science Robotics*, vol. 1, no. 1, 2016, art. no. eaai7529.

[17] Z. Ding, C. Wang, K. Liu, J. Jiang, D. Yang, G. Pan, Z. Pu, and T. Liu, "Distributed optical fiber sensors based on optical frequency domain reflectometry: A review," *Sensors*, vol. 18, no. 4, pp.1072, 2018.

[18] J. Guo, M. Niu, and C. Yang, Highly flexible and stretchable optical strain sensing for human motion detection, Optica, vol. 4, no. 10, pp. 1285-1288, 2017.

[19] A.Leber, B. Cholst, J. Sandt, N. Vogel, and M. Kolle, Stretchable thermoplastic elastomer optical fibers for sensing of extreme deformations, Advanced Functional Materials, vol. 29, no. 5, pp. 1802629, 2019.

[20] H. Souri, H. Banerjee, A. Jusufi, N. Radacsi, A.A. Stokes, I. Park, M. Sitti, and M. Amjadi, "Wearable and stretchable strain sensors: Materials, sensing mechanisms, and applications," *Advanced Intelligent Systems*, vol. 2, no. 8, pp. 2000039, 2020.

[21] C. Larson, B. Peele, S. Li, S. Robinson, M. Toraro, L. Beccai, B. Mazzolai, and R. "Shepherd, Highly stretchable electroluminescent skin for optical signaling and tactile sensing," *Science*, vol. 351, no. 6277, pp. 1071-1074, 2016.

[22] J. Guo, X. Liu, N. Jiang, A.K. Yetisen, H. Yuk, C. Yang, A.Khademhosseini, X. Zhao, and S.H. Yun, "Highly stretchable, strain sensing hydrogel optical fibers," *Advanced Materials (Deerfield Beach, Fla.)*, vol. 28, no. 46, pp. 10244, 2016.

[23] Z. Liu, Z. Li, and L. Cheng, "A two-dimensional reticular core optical waveguide sensor for tactile and positioning sensing," in *IEEE/RSJ International Conference on Intelligent Robots and Systems (IROS)*, 2023, pp. 8937-8942.

[24] J. Guo, M. Niu, and C. Yang, "Highly flexible and stretchable optical strain sensing for human motion detection," *Optica*, vol. 4, no. 10, pp. 1285-1288, 2017.

[25] D. Wang, B. Sheng, L. Peng, Y. Huang, and Z. Ni, "Flexible and optical fiber sensors composited by graphene and PDMS for motion detection," *Polymers*, vol. 11, no. 9, pp. 1433, 2019.